Printability of ABS-HDPE Blended Virgin Filaments

Uladzimir Kasacheuski[1,2], Laura Luther[3,5], Qiuyu Deng[3], Jinyun Zhou[3],
Amanda Siegel[4,6], Andres Tovar[3,6]

[1]Department of Physics, IUPUI School of Science; [2]Department of Computer Science, IUPUI School of Science; [3]Department of Mechanical Engineering, Purdue School of Engineering and Technology; [4]Department of Chemistry and Chemical Biology, IUPUI School of Science; [5]Department of Chemistry, Butler University College of Liberal Arts and Sciences; [6]Integrated Nanosystems Development Institute, IUPUI

Abstract

The purpose of this research is to determine the printability of ABS/HDPE blends for fused filament fabrication (FFF) additive manufacturing (AM). Achieving a highly printable blend of ABS/HDPE would open the doors to an effective method of recycling HDPE and ABS plastics. Currently, the printability of HDPE (High Density Polyethylene), one of the most widely commercially used plastics in the world, is very low and the material is not an effective choice for most FFF printing scenarios. To improve the printability of HDPE, we add ABS (Acrylonitrile Butadiene Styrene), a material with high printability and which is commonly used in FFF. In this study, we define the properties that determine FFF printability and the parameters that affect these properties. We then analyze the printability of four blends of ABS/HDPE.

The blend ratios analyzed in this study are 0%, 25%, 50%, 75%, and 100% HDPE by weight. The virgin states of the plastics are examined to distinguish virgin pure and blend properties. The chemical characteristics of the filaments and their products are determined using Fourier transform-infrared spectroscopy (FTIR) and field emission scanning electron microscope (FESEM). The mechanical characteristics of the materials are determined by tensile testing. These chemical and mechanical properties demonstrate the printability of the material.

The results show that 50%wt HDPE is the most promising blend of ABS and HDPE, with ease of printing, minimal warping, as well as comparable speed and strength to pure ABS. FTIR and FESEM results show that ABS and HDPE are immiscible when blended but still homogeneously fill the material. These chemical properties decrease the printability of the material at 25%wt and 75%wt HDPE and maximize the printability at 50%wt, as evident by the resultant mechanical properties of the blends. Future work may consist of analyzing the effects of additives or further 'tuning' of the ratios can lead to an even more printable blend.

1 Introduction

In light of sustainability and the gaining momentum of 3D printing in today's world, our research delves into the possibility of recycling commonly used thermoplastics for use in FDM printing. We begin our research by defining which qualities are required for a material to be suitable for 3D printing and defining the parameters that can affect 3D printing material printability. Although there has been much research determining the printability of blends and additives for 3D printing, with references 11-22 being a few of *many*, a systematic and thorough process of characterizing a material to determine its printability for 3D printing has not yet been defined or standardized. In this research we define the foundation for a full and thorough characterization process and implement it in the study of two materials blended together at different ratios.

The ability to recycle plastic for extrusion-based additive manufacturing is largely determined by its printability. While the plastic printability depends heavily on the additive manufacturing unit (3D printer), this can be assessed based on five key features that are common to all extrusion-based system: (1) liquification of the material, (2) extrusion power, (3) quality of the extruded filament, (4) solidification, and (5) bonding of the material to itself and to a substrate. These key features are ultimately determined by the thermal, mechanical, and chemical properties of the material. In addition to this, the environmental properties should be considered for health and sustainability impacts, qualifying more on the terms of a logistic difficulty as opposed to an engineering difficulty associated with the printing of a material.

The thermal properties of the material, such as glass transition temperature, melt-flow index (MFI)[1], thermal conductivity, and thermal expansion, play a significant role in extrusion-based additive manufacturing such as fused filament fabrication (FFF). FFF works on the principle that solid plastic in the form of filament or pellet becomes liquid in a heated chamber and then can be pushed and ejected through a die or nozzle. The heat to the chamber is normally applied through heating coils, which maintain a constant temperature during the melting process. The larger the chamber and/or the higher the temperature, the more difficult this process can become—plastics tend to burn or degrade at high temperature and the cooling process following the extrusion becomes a problematic. The glass transition temperature can be used to assess what kind of printer parameters are required to melt the material for extrusion. The MFI would be useful in determining the force required to extrude a material and ensuring a consistent flow rate. Thermal conductivity and thermal expansion would be critical in predicting a material's tendency for warpage and assessing the requirements to minimize this warpage, such as a heated printing chamber. [Add literature review]

The mechanical properties of a material such as its elastic, plastic, and fracture properties are of interest when assessing the printability a filament. Not only are the mechanical properties of a material are of great interest for functional prototype and production focused FFF, as evident by ample research[18-29], but these properties, such as the brittleness and flexibility, can dramatically affect the reliability printer working with the material throughout the extrusion process. [Add literature review]

The printability of a material can be directly influenced by the material's chemical characteristics and composition and will directly influence the design parameters and printing parameters used when printing with the material. In addition to this, while thermal properties and environmental properties are manipulated solely by a materials composition, the mechanical properties of the 3D printed product can be manipulated all three parameter sets which is significant for the end use of the material. Material composition can be manipulated by blending two or more plastics at defined ratio compositions (mole or weight ratio) and can be affected by additives in a material, including the increasingly popular

nanoparticles such as carbon nanotubes[11] and even metals[13]. Material composition parameters directly affect the chemical characteristics of a material and can fundamentally change the material's properties. [Add literature review]

Environmental properties such as fume toxicity, degradation period, recyclability are worthwhile to be assessed as well. Fume toxicity is worth understanding for the direct hazards presented in research and manufacturing environments where plastic is melted. The degradation period of a material as well as what methods can be used to break the plastic down are of interest for the end of life sustainability of this material, in order to limit the pollution that our manufacturing creates. The recyclability of the material is of interest in order to assess the potential of closing the end of life for products made with the material; distinctly worthwhile for non-renewable resource based plastics like petroleum, this is a method of increasing the sustainability of the resource. [Add literature review]

The objective of this research is to …. Due to the endless amount of materials that can be made by blending different materials as well as using additives like nanoparticles[11,13], we narrowed the scope of our research to ABS and HDPE and employed the characterization process to determine if they together will make a suitable filament for use in fused deposition modeling (FDM). HDPE has shown itself to not be great for 3D printing, but because of its proliferation in accessible consumer products, the ability to employ this plastic in 3D printing would create a sustainable end of life for HDPE consumer goods. We hypothesize that combining HDPE with ABS will improve the properties of HDPE for 3D printing. ABS and HDPE are great materials to use for this research because they are both thermoplastics. Thermoplastics are capable of being heated and cooled multiple times and display the same characteristics as before it was ever heated. For example, most of the plastics in our lives, from bottles (HDPE) to bottle caps (PP), are petroleum based products. Unfortunately, petroleum is the textbook example of an unsustainable resource. Petroleum is not a renewable resource and its reserves are distinctly finite[9]. In addition to being an unsustainable resource, the common end of life of this product is equally unsustainable; for example, HDPE takes more than 450 years for it to degrade in the environment[4].

In this study, blends of ABS and HDPE were created and extruded into filament and were used to print with. Ratios of 0%, 25%, 50%, 75%, and 100% HDPE were created, where 25% refers to a blend of 25%wt HDPE and 75%wt ABS. After the creation of the blended material filaments, the blended materials were chemically characterized using FTIR and FESEM. The blended material filaments were then printed with an FFF printer into modified tensile test specimens. The materials were chemically characterized using FTIR and FESEM. The printed specimens were used in tensile tests for mechanical characterization. The study produces quantitative as well as qualitative printability results about the blended materials as they go through the process.

2 Chemical Characterization of ABS/HDPE blends

Note: they appear to be miscible: http://reprap.org/wiki/ABS_HDPE_blend

2.1 Specimen preparation

In characterizing a material chemically we employ the techniques of FTIR (Fourier transform-infrared spectroscopy) and FESEM (field emission scanning electron microscope). The FTIR enables the observation of the functional groups of a compound and can be used to determine if two materials are

miscible and form a new molecule through the blending process. FESEM enables the observation of the atoms and their distribution. Employing FTIR throughout the material lifecycle can be used to confirm the thermoplasticity of blended and raw materials.

FTIR is conducted on multiple distinct materials throughout this research for as thorough of a chemical characterization as possible. A Thermo Scientific Nicolet iS10 FTIR machine is used to run all FTIR analysis.

The FTIR of pure ABS pellets, pure ABS filament, pure ABS printed product, pure HDPE pellets, pure HDPE filament, 25%wt HDPE filament, 50%wt HDPE filament, and 75%wt HDPE filament was conducted. Both the methods of dissolving the materials and filling the materials were explored for FTIR. In the end, FTIR was conducted by dissolving the material of interest and drying the resulting solution on a KBr (Potassium Bromide) tablet, which is then used to conduct FTIR. Due to the difficulty of finding a method to obtain a sample small enough of FTIR analysis, both by dissolution and filling, only the pure ABS, pure HDPE, and 25%wt HDPE material was successfully analysed by FTIR.

The pure ABS materials (pellets, filament, and printed product) dissolved with acetone producing a slurry, milky solution. The solution was dropcasted onto a KBr (Potassium Bromide) tablet ensuring that the KBr tablet was completely covered with a thin film of the solution. After ensuring that no acetone is left, the test sample is then loaded into the machine and the test is conducted.

The pure HDPE pellets and filament were dissolved with more difficulty**.** Dissolving HDPE required the use of chlorobenzene and sonification for a period of 5 days. While this did not fully dissolve the HDPE, enough of the material was dissolved for FTIR testing. From here, a similar process as with the ABS solution was conducted for FTIR analysis of the HDPE pellets and filament.

25%wt HDPE was dissolved with toluene under the knowledge that toluene would dissolve both HDPE and ABS better than what chlorobenzene would[2,3]. The solution was rod sonicated with Branson Digital Sonicator at 50% amplitude for 7 minutes. The filament did not completely dissolve, but enough dissolved to prepare a sample for FTIR based on the change in color from clear to cloudy. The standard analysis procedure was used to obtain FTIR results on this solution.

Figure 3. Left test tube: Pure chlorobenzene, Right testtube: Chlorobenzene with partially dissolved filament

The FTIR of the 50%wt HDPE and the 75%wt HDPE was not successfully conducted, due to the inability to successfully dissolve both components of the blend. Both Toluene combined with the sonication as well as Chlorobenzene with heatgun were used to attempt to create usable solutions of the material. In the case of Toluene, neither material dissolved. In the case of chlorobenzene, only the peaks of HDPE appeared in the FTIR analysis with no trace of ABS. This demonstrated that both Chlorobenzene was not a good solvent to use for a blend of HDPE and ABS.

2.2 FTIR

The peaks of pure ABS are characterized by functional groups based on the IR spectrum and compound that is analyzed. The Acrylonitrile is characterized by the CN bond at about 2238 cm^{-1}. The Butadiene is represented by the 966 cm^{-1} peak and the Styrene is characterized by the benzene group and represented by the 1601 cm^{-1} peak[4]. Pure HDPE characterized by the peaks found just under 3000 cm^{-1}, around 1500 cm^{-1}, and between 700-750 cm^{-1}. The two peaks represented by 2916.88 cm^{-1} and 2848.59 cm^{-1} are characterized by the CH_2 asymmetric stretching while the 1472.61 cm^{-1} and 1462.32 cm^{-1} are bending deformation seen. The peak in the range of 700- 750 cm^{-1} represents a rocking deformation found in HDPE[6]. The FTIR results for pure ABS and pure HDPE verify the thermoplasticity of the materials and serve as an important benchmark for analyzing the effects of blending the two materials.

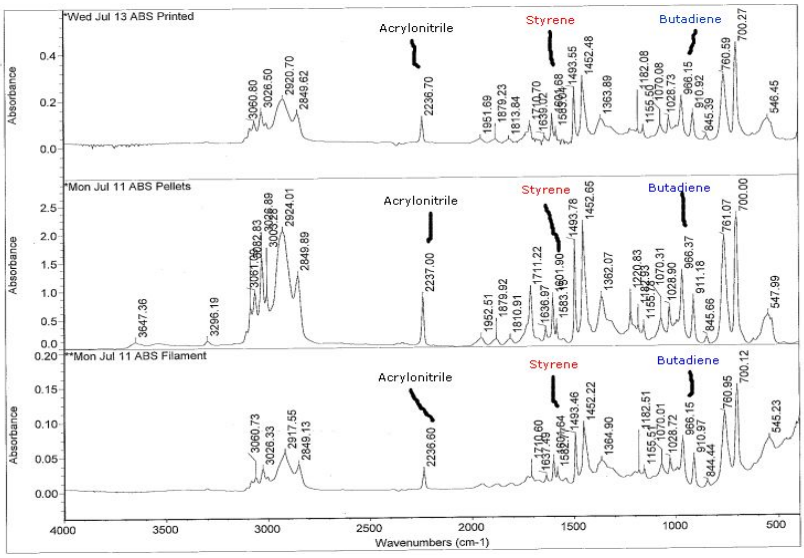

Figure 7. FTIR results of ABS pellets, filament, and printed dissolved in acetone

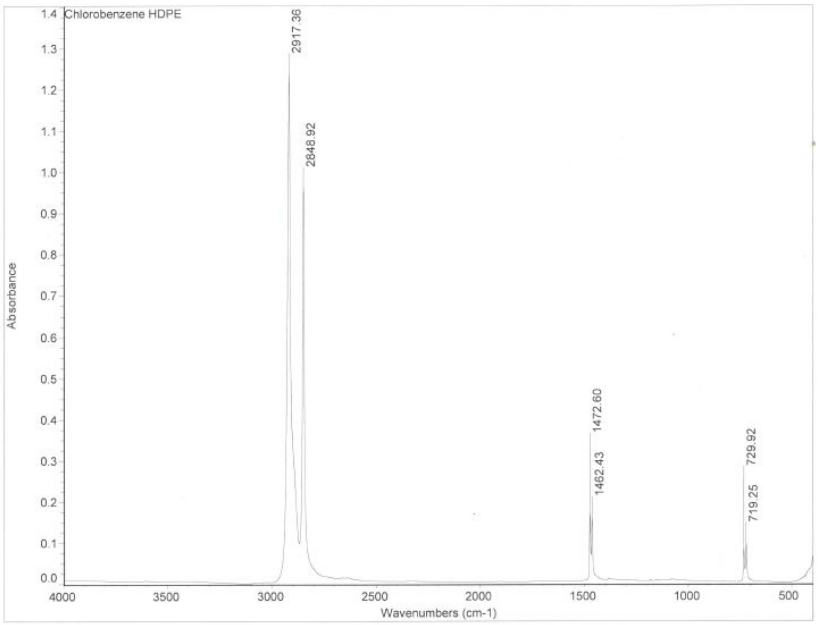

Figure 8. FTIR results of pure HDPE dissolved in chlorobenzene

The FTIR analysis for the 25%wt HDPE blend is shown below in figure 9, compared to the results of pure ABS and pure HDPE. Interpreting the results, it can be seen that there are no band shifts seen in the blended filament. The peaks seen can be easily determined as ABS or HDPE, which indicates that ABS and HDPE are immiscible. It is also important to point at that the intensity of some peaks changed in the blend, such as the Acrylonitrile peak, 2236.71 cm^{-1}, drastically decreased in intensity in the blend and the peak at 1452.81 cm^{-1} also decreased. It is hard to determine the HDPE present in the blend as the peaks that define HDPE seem to overlap in the same regions that ABS resides. This is due to the fact that ABS and HDPE are very similar in structure with the exception of the triple bond CN in ABS at about 2236.71 cm^{-1} in the blend. One area they overlap is the peak of 2921.16 cm^{-1} which is comprised of some signal from ABS as well as HDPE.

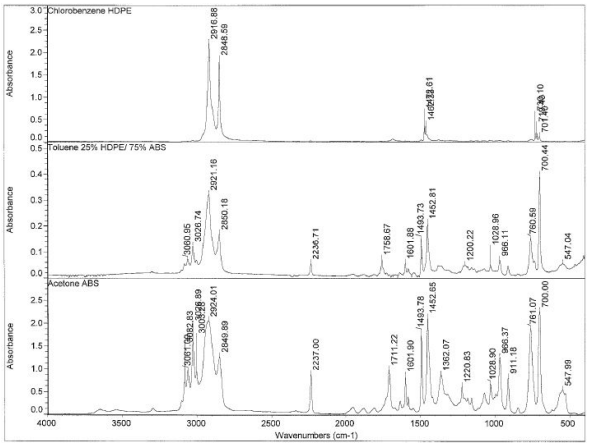

Figure 9. FTIR results pure ABS dissolved in acetone, pure HDPE dissolved in chlorobenzene and blended 25% wt HDPE/ 75% wt ABS dissolved in toluene

2.3 FESEM

FESEM was run on 50 wt% HDPE, pure ABS, and pure HDPE. The results show that the 50%wt blend has a rough texture but is homogeneous throughout. The rough texture could indicate that certain areas of the filament are clumping together and are not evenly dispersed throughout the filament resulting in the two plastics not interacting. However, closer inspection demonstrated that nitrogen was found evenly dispersed in the filament. Considering that ABS has the only nitrogen present in the blend, this indicates that, on at least some level, the plastics are blending. We believe that the FESEM shows us that these two plastics are, more likely than not, overlapping one another and not thoroughly mixing with each other. These results match up with the results seen from the FTIR: even though the blend seems to be evenly dispersed they remain immiscible.

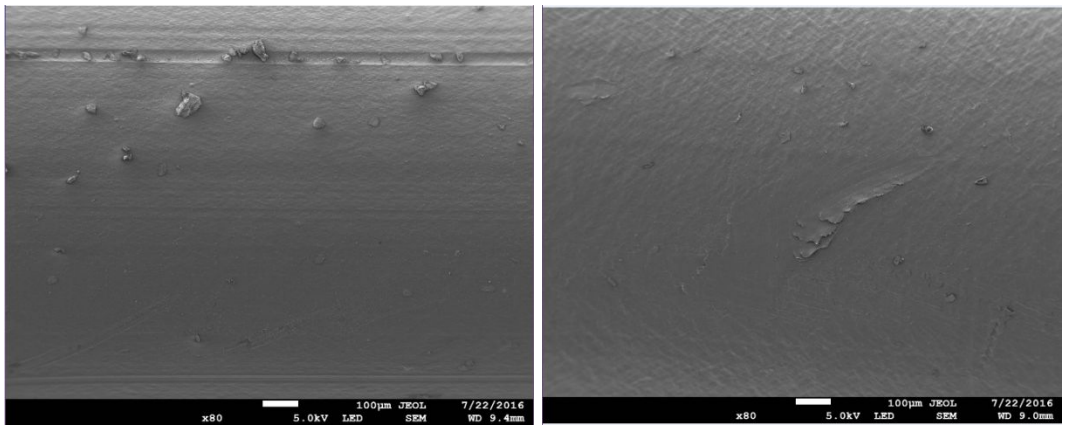

(a) (b)

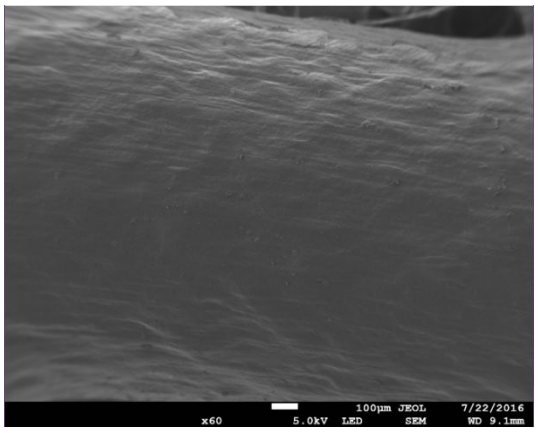

(c)

Figure 11. FESEM results of filaments extruded in lab (a) pure ABS filament showing surface at x80 magnification at 100 µm (b) pure HDPE filament showing surface at x80 magnification at 100 µm (c) 50% wt HDPE/50% wt ABS blend showing rough but homogeneous surface

3 Mechanical characterization of ABS/HDPE 3D-printed specimens

3.1 Material Fabrication and Filament Extrusion

The results of the extrusion and printing process show that the filament created by 25%wt HDPE is qualitatively much more brittle than both pure ABS and pure HDPE. Based on the results of the chemical characterization, we believe that the immiscibility of the two blends decreases bonding of the overall material and that this effect is most prominent when too much HDPE exists in the blend. **Can we hypothesise that because HDPE is more plastic and ABS is more brittle, higher percentages of HDPE mitigate the effects of immiscibility on the material's brittleness which ABS does not accomplish this as well?**

3.2 Filament Fabrication

In this study, pure ABS and HDPE were sourced in pellet forms and then extruded into filaments. The ABS used was a MG94 ABS CYCOLAC Resin Pellets by Sabic (Pittsfield, MA). The ABS pellets were obtained from Sabic's CYCOLAC Resins in the color white.. The HDPE used used was from Professional Plastics, Inc and purchased from 3Dprinterstuff.com in the color white. The pellets are roughly around 5 mm in diameter.

Different blends of ABS and HDPE were made by weight percentages of 0%, 25%, 50%, 75%, and 100% HDPE. After creating and mixing a blend by weight percentage, the pellets are placed in an oven with 70 °C for 24h to reduce the moisture content of the material, increasing the consistency of the filament extrusion process. The mixed and moisture reduced pellets are then extruded in a Do-It-Yourself extruder, the "Filastruder", which runs at around 12v DC, 8 rpm, 15.6 N-m torque. The extrusion process was used to create a filament of 1.75mm in diameter which is a popular diameter used by most 3d printers.

During the extrusion process, speed of extrusion and filament diameter stability were optimized for by adjusting extrusion temperature. In our extruder, RPM and extrusion rate were variables dependent variables controlled by the PWM board. The board increased the torque, and consequently the extrusion rate and diameter, depending on the viscosity of the material in the extruder. We are able to control extrusion temperature, which affects these dependent properties. As the MFI of the HDPE is much lower than ABS and requires more torque to extrude, we increased the extruding temperature with the increase of the ratio of HDPE in the blend. This rise in temperature increases the extrusion rate; however, the extrusion of filament with HDPE is still slower than that of virgin ABS.

Filament diameter is stabilized at 1.75mm ±0.02mm by applying tension by means of a filament winder and enforced by checking the diameter by IR and physical tubes. The system we used for filament winding and diameter enforcement was the Do-It-Yourself extruder, the "FilaWinder", sold by the company "Filastruder". Table 1 displays the final optimal parameters in found for the extrusion of various blends of ABS to HDPE.

Material(ABS:HDPE)	Extruding Temperature(°C)	RPM	Motor current-Torque related(A)	Extrusion rate(mm/min)

100:0	180	8	0.6	827.2
75:25	210	8	0.54	434.6
50:50	230	8	0.60	257.2
25:75	250	8	0.63	217.4
0:100	270	8	0.66	139.6

Table 1. Transversely Isotropic Material Compliance Matrix

3.3 Printing of Blended Material

After creating a filament for each blend, the new blended material filament is used for FFF printing. The printing is conducted using a RepRap I2 3D printing machine. Each blend was to be printed in three orientations of a standard testing specimen for use in mechanical characterization. The specimen model is a modified ASTM Standard D638 using the type IV dimensions. The raster pattern is defined by a [0, 90] stacking sequence. We print the specimens in the three build orientations demonstrated in figure 1: O_1, O_2, and O_3. O_1 is printed "standing up" and is to be tested along the z-axis. O_2 is printed on the build plane, to be tested along either the X or the Y axis. O_3 is printed as O_1 rotated 45 degrees away from the z-axis on either the XZ plane or the YZ plane.

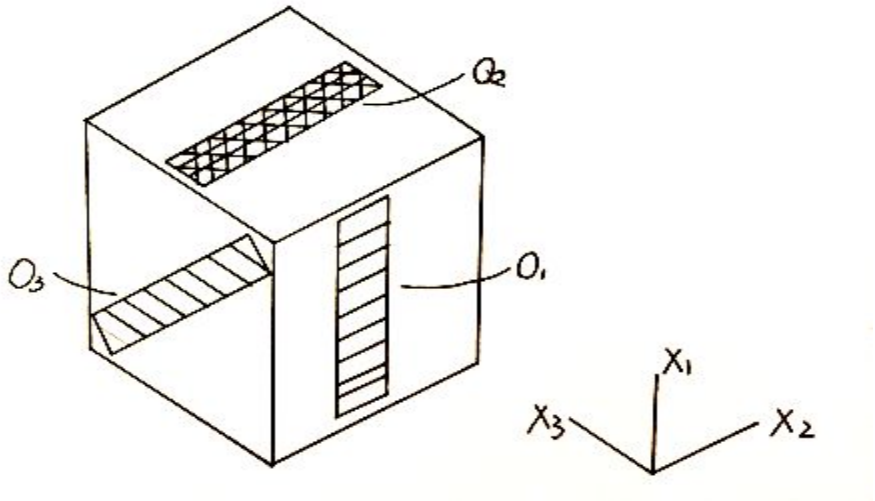

Figure 1. Demonstration of three build orientations.

For each orientation and each blend we attempted to print 4 specimens. Unsurprisingly, the printing of ABS specimens progressed with no difficulties, ***(Figure (X-1)a-b)***. The printing of 50%wt HDPE was the most successful printing set containing HDPE. Beyond this, the printing of the 3 remaining blends, 25%wt HDPE, 75%wt HDPE, and 100%wt HDPE were plagued with printing problems. Ultimately,

successful printing of specimens for mechanical characterization was only achieved for 0%wt HDPE and 50%wt HDPE.

The REPRAP printer used had a nozzle diameter of 0.35mm. The diameter of all filaments used was 1.7mm. For both blends and pure materials, the printing temperature was kept constant at 240C in the extruder and a bed temperature of 120C. For both blends and pure materials, the default extrusion width was 130%. For pure ABS, layer thickness was deposited at 0.35mm. For HDPE blends, layer thickness was deposited at 0.55mm.

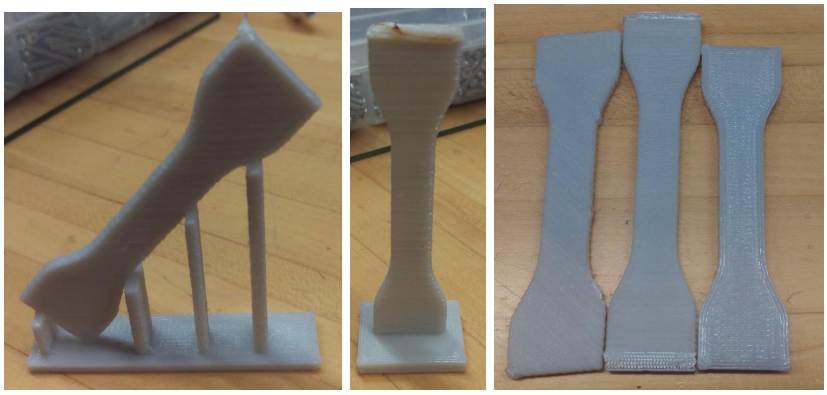

Figure X - a) Printed ABS O_3 specimen. b) Printed ABS O_1 specimen. c) Side by side comparison of specimen O_3, O_1, and O_2 in order from left to right. We believe the discrepancies in the size to be caused by the slicing software used, Slic3r.

When printing 25%wt HDPE, a distinct initial surprise displayed itself: the rate of jamming in the printer was significantly higher than expected. In attempting to print these filaments, the filaments will undergo brittle failure, ***fracture at the pulling gear,*** and jam the extruder too often to fully create a product. The gear meant to be driving the filament through the extruder will instead carve out a section of the filament, loose grip of the filament, and rotate indefinitely - 'jamming' the printer. The brittleness of the filament surprising because both the pure ABS and especially the pure HDPE are much more plastic than the blend. ***We believe this brittleness can be explained by the chemical properties of the material.***

The finicky properties of higher ratios of HDPE, 25%wt and above, in printing presented themselves prominently through thermal warping, as shown in **Figure X**, under standard printing process parameters. This tendency to undergo thermal warping increases as the %wt of HDPE increases, which is reasonable considering the temperature expansion coefficient of HDPE (120.0 10^{-6} m/m ^{o}C) is approximately twice that of ABS (63.0 10^{-6} m/m ^{o}C) ***[Do we need to cite engineering toolbox for the t.e.c?]***. The thermal warping can be managed and minimized by printing process parameters: we found that by modifying road width, layer thickness, and printing speed we were able to dramatically mitigate the effects of the warping of the 3D printed object. A lower speed, for example reducing infill and perimeter print move speed from 50mm/s to 20mm/s, decreases the warping marginally; however, increasing the road width or increasing the layer thickness both practically eliminated the warping. ***We believe that this warping could be a factor of thermal warping and potentially even of a highly malleable material being "pulled on" by a viscous extruded filament***. **Figure Xb** demonstrates the

minimal warping of a 50%wt HDPE O_2 specimen when printed under tailored printing process parameters.

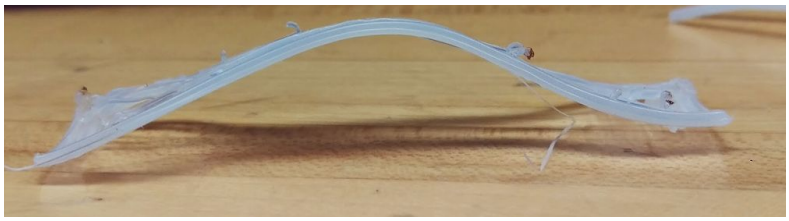

Figure X - A display of the prominent thermal warping undergone by an aborted 50%wt HDPE O_2 specimen under average printing process parameters.

Figure Xb - A display of the minimal thermal warping undergone by a 50%wt HDPE O_2 specimen under tailored printing process parameters.

For the printing of 50%wt specimens we utilized the tailored printing process parameters. Even so, successful printing of O_1 and O_3 specimens were not feasible with the 50%wt HDPE blend. We found that HDPE takes much longer to transition out of a malleable state. **Figure Xa** shows a 50%wt HDPE specimen after cooling down without "flattening". **Figure Xb** shows another 50%wt HDPE specimen, with the same design and printing process parameters, after cooling down with "flattening". It is clear that the specimen is still quite malleable after printing for some time.The longer cooling time of HDPE combined with the smaller laminar printing area of the O_1 and O_3 specimens made printing the O_1 and O_3 specimens unfeasible. The print was aborted without exception either due to warping of the specimen or disadhesion of a newly extruded path during each attempt, and was interpreted as a demonstration that the 50%wt HDPE filament was still not as easily printable as pure ABS.

Figure Xa - 50%wt HDPE O_2 specimen after cooling down without "flattening"

Figure Xb - 50%wt HDPE O_2 specimen after cooling down with "flattening"

At 75%wt HDPE and 100%wt HDPE, the filament itself is not suitable for printing in the REPRAP as it is too flexible; when printing instead of entering the extruder the pure HDPE filament instead snakes around the entry and jamming in this way, demonstrated in ***Figure X+1***. The frequency of this snaking

and jamming occurs too regularly to create a successful print. While reducing printing speed will reduce the chance that this happens, it does not prevent it.

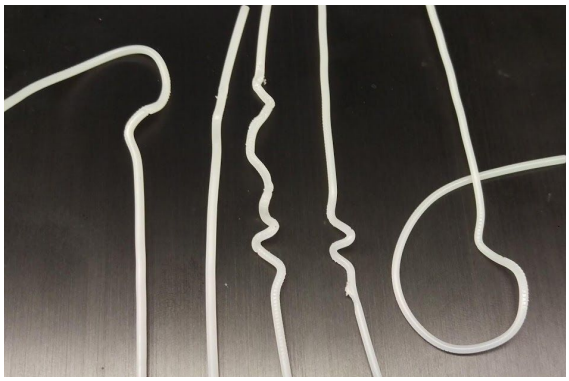

Figure X+1 - Examples of the 100%wt HDPE filament ‘snaking’ due to its plasticity

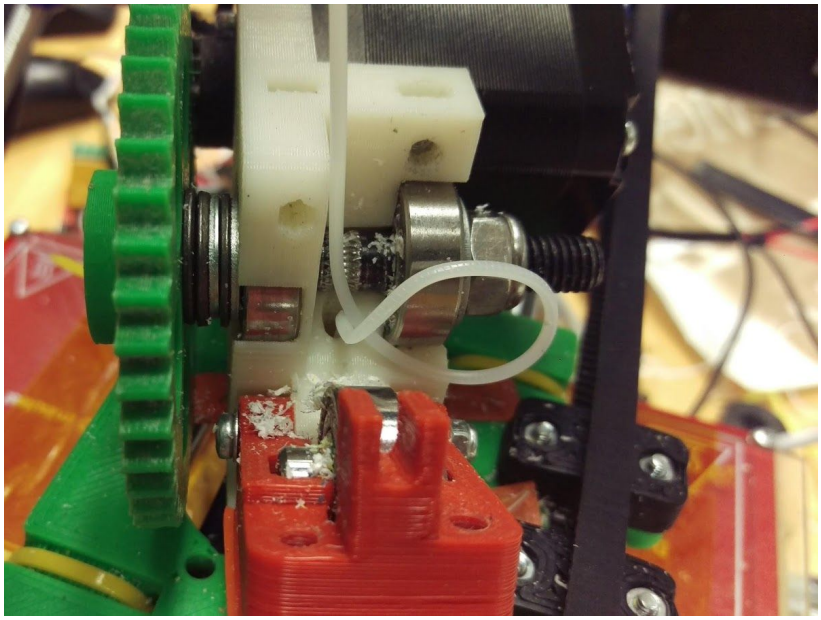

Figure X+2 - Example of the 100%wt HDPE filament jamming the printer due to ‘snaking’

3.4 Tensile test

In characterizing a material mechanically we employ the process of tensile testing several explicitly defined specimens of the material. Through the results generated by tensile tests we are able to determine elastic, plastic, and fracture properties described by the stress-strain curve. It must be noted that because the mechanical strength of a printed product greatly depends on how the material was printed, the results generated by testing products should be considered relative to other results with equivalent design and printing parameters, as opposed to absolute values. Still comparing with absolute values may be informative.

The mechanical characterization is based on results generated by tensile tests. Tensile testing was conducted on a MTS Q-Test Machine (USA, MN), (see Figure 4). Before testing, the gauge width, gauge depth, and separation distance was recorded. An extensometer was used to measure specimen

elongation. This machine was equipped an MTS extensometer model 634.12E-54. Data points were collected at 5 Hz**.** Standard engineering stress/strain equations were used to calculate stress and strain for both of these tests types by MTS provided software, TestWorks 4. Stress-strain curves with significant data points were generated for every specimen that was successfully produced.

Figure 4. Tensile Testing Setup

Tensile tests were conducted smoothly on the aforementioned MTS tensile tester with extensometer. Almost all testable specimens that were created were successfully tested. ***Figure Z2*** demonstrates an example of the stress/strain curve generated in TestWorks 4 during tensile testing. While extrusion width decreases thermal warping in HDPE, a large extrusion width created specimens that were not feasible tensile test specimens, as demonstrated in **Figure Z**. Specimens with thinner road widths while still minimized warping were later used for the testing of O_2 50%wt HDPE.

Figure Z-1 - Successful O_2 pure ABS specimen after completion of a tensile test, with specimen still in test setup.

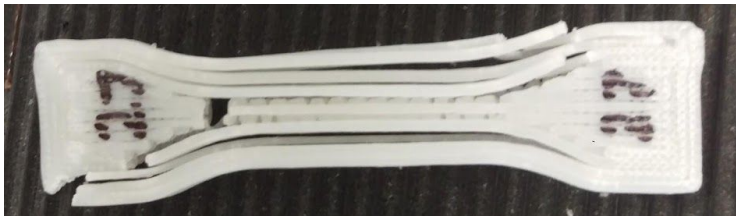

Figure Z - A O_2 specimen with road width 200% fractures at the perimeter when printed at our specified specimen dimensions. Because this perimeter takes up such a large volume of the specimen and knocks the extensometer loose upon fracture, specimens with 200% road with are not feasible for tensile testing in our context.

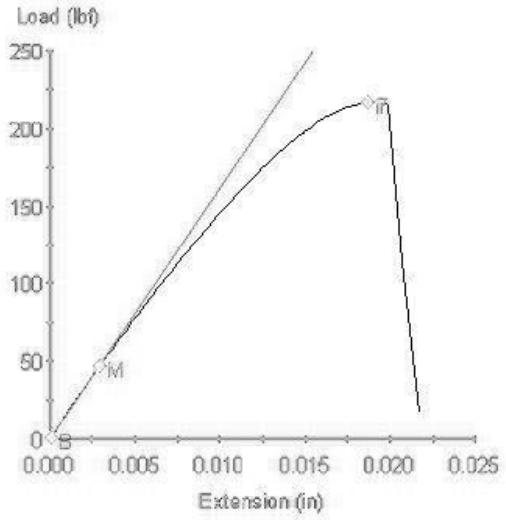

Figure Z2 - Example of a stress/strain curve generated by TestWorks 4 from the data of a tensile test of specimen O_2, pure ABS.

The results of the tensile tests are displayed in **Table X** displays the results of the successful tensile tests. The results of pure ABS and 50%wt HDPE in the O_2 orientation compared to known values of the elastic modulus and ultimate strength for pure ABS and pure HDPE is shown in **Table Y**.

When comparing the elastic moduli of the materials, referring to **table y**, we find that the blend 50%wt HDPE has an elastic modulus much larger than of pure HDPE, and one that is within the bounds of the known values for pure ABS. This is a surprising finding when acknowledging that only 50% of the material by weight is ABS, but does explain why we do not experience jamming due to 'snaking' in the printer head as we experience with 75%wt and 100%wt HDPE. When interpreting the Ultimate strength of 50%wt HDPE to both pure ABS and pure HDPE, we must recognize that the ultimate strength of the pure ABS specimens we printed were all lower than the known pure ABS value. This is most likely a product of the laminar nature of FFF printed materials. With this consideration, it is more informative to notice that the difference between the ultimate strengths of the pure, known values, of ABS and HDPE is 3.62 ksi. However, the difference between the average ultimate strength values of the pure ABS FFF specimen and the 50%wt HDPE FFF specimen is 1.58 ksi. This is closer to 50% of the difference from the

pure blends and resembles a more linear relationship between the %wt of each component and their contribution to the overall value.

These results show to us that the printability of the 50%wt HDPE blend is larger than of pure HDPE, due to the increased elastic modulus. These results also show us that the ultimate strength of the blended material is improved when we have a 50%wt ratio of the stronger material, ABS.

Material	Orientation	Elastic Modulus **(ksi)**	Ultimate Strength **(ksi)**
Pure ABS	O_1	222.7320 ± 10.9630	1.0065 ± 0.1039
Pure ABS	O_2	238.8737 ± 8.1610	3.276 ± 0.2217
Pure ABS	O_3	226.9760 ± 26.4698	1.7 ± 0.4243
50%wt HDPE	O_2	203.2902 ± 32.6952	1.9715 ± 0.5384

Table X - Elastic modulus and ultimate tensile strength calculated for all 3 pure ABS orientated and for O_2 50%wt HDPE specimens.

Source	Material	Elastic Modulus **(ksi)**	Ultimate Strength **(ksi)**
measured	Pure ABS	238.9 ± 8.2	3.28 ± 0.22
known	Pure ABS	203.1 to 449.6	5.80
measured	50%wt HDPE	227.0 ± 26.5	1.70 ± 0.42
known	Pure HDPE	116.0	2.18

Table Y - Elastic modulus and ultimate strength for FFF printed pure ABS and 50%wt HDPE both in the O_2 orientation compared to the known elastic modulus and ultimate strength of the materials.

Would be useful to measure the elastic modulus and Ultimate Strength of pure HDPE, 75%HDPE, a 25%HDPE filaments we created. Could be done by forgoing printing and simply measuring the filaments. Perhaps, data anomalies can also be reduced by forgoing the laminar and printing process parameter contributions of mechanical properties on a material.

4 Conclusion

Overwhelmingly, the work has demonstrated that while blends of ABS/HDPE are not as printable as pure ABS, which is expected, the blend of 50%wt HDPE is the superior blend in comparison to 25%wt, 75%wt,

and 100%wt HDPE. This result leaves the door open for further optimization of ABS/HDPE blends and shows that printable blends of HDPE are feasible.

In this study, we created filaments of 5 blends of ABS and HDPE, conducted chemical characterization on the materials, printed the materials, and conducted mechanical characterization on the printed parts. Throughout the study, we've found that the printability of HDPE can be optimized at a blend ratio of 50% HDPE by weight. The chemical characterization demonstrates that although ABS and HDPE are immiscible, they homogeneously distribute themselves across the material. The mechanical characterization demonstrates that at 50%wt HDPE, the elastic modulus of the material closely resembles the elastic modulus of the highly printable ABS, which represents a decreased risk of the filament jamming the printer and increases the printability of the HDPE. We have also found that at 50%wt HDPE, the ultimate tensile strength of the material is improved beyond the ultimate strength of pure HDPE. Most surprisingly, we've found that the printability of HDPE does not increase linearly with the increase of the highly printable ABS: 25%wt HDPE is in fact one of the least printable blends we had tested.

These findings demonstrate that the printability of HDPE can be optimized by blending the material with more printable material. Specifically, this demonstrates that ABS can be successfully used to increase the printability of HDPE. These findings also demonstrate that increasing the printability of HDPE is not trivial: a higher ratio of a highly printable material does not correlate to a higher printability of the product material. This paper demonstrates a method by which the printability of a material can be assessed, an example of the printability of HDPE being improved, a starting point for further optimization of HDPE printability, and lessons learned on how to more efficiently conduct this process. With these findings, we are one step closer to finding a more sustainable alternative to the end of life of HDPE.

Future work for optimizing the printability of HDPE will include `fine tuning` of the blend ratios, examining the printability of ratios between 30%wt HDPE and 70%wt HDPE. In addition to this, we believe the consideration of additives to the blends may prove to have notable effects on the printability of the blend. Future work will also consist of conducting FTIR on the materials by the 'pressing' technique, as opposed to dissolving the materials, as this would be more reliable and remove the possibility of dissolving bonds between the blended ABS and HDPE material. We recognize that a limitation of this work was the mechanical characterization of the FFF printed products of the materials without the characterization of their respective filaments. By characterizing the mechanical properties of the filaments, we would gain a more direct understanding of the materials properties and not be limited by the poor printability of materials we wish to analyze. Finally, the analysis of thermal properties would bring a significant insight into the printability of a material due to the problems of thermal warping.

5 Acknowledgements

The authors thank INDI (Integrated Nanosystems Development Institute) for the use of their labs and equipment and Dan Minner for helping with the FESEM portion and the pressing method for creating KBr tablets with blended material. We thank Ali Daneshkhah for teaching us how to use the equipment available in the INDI labs, as well as, providing materials and solvents when needed. We also thank Dr. Mangi Lalagarwal for all his support and help during this research. We also thank Arturo Garcia for his availability and help in maintaining the RepRap machines as well as offering advice in the Additive

Manufacturing lab. We also thank Sandeep Korupolu for being generous with time and knowledge throughout the mechanical testing processes.

6 References

[1] Peydro, M. A., Juarez, D., et al. (2013, May). Study Of The Thermal Properties Of Acrylonitrile Butadiene Styrene – High Impact Polystyrene Blends With Styrene Ethylene Butylene Styrene. ANNALS OF THE ORADEA UNIVERSITY. Fascicle of Management and Technological Engineering. AUO FMTE, XXII (XII), 2013/1(1), 273-276. doi:10.15660/auofmte.2013-1.2827

[2] Rehau. (213, February). Acrylonitrile-butadiene-styrene (RAU-ABS). Retrieved July 19, 2016, from https://www.rehau.com/download/1465460/materialmerkblattrau-abs-en.pdf

[3] Professional Plastics. (n.d.). HDPE and LDPE Resistance Chart by Chemical. Retrieved July 19, 2016, from https://www.professionalplastics.com/professionalplastics/HDPE-LDPEChemicalResistanceChart.pdf

[4] Hamod, H. (2014, December 1). Printability of recycled HDPE for 3D printing filament (Unpublished master's thesis, 2014). Arcada University of Applied Science. Retrieved July 1, 2016, from https://www.theseus.fi/bitstream/handle/10024/86198/Thesis final.pdf?sequenc

[5] Albano de Morais, J., Gadioli, R., & Aurelio De Paoli, M. (2016, June 7). Curaua fiber reinforced high-density polyethylene composites: Effect of impact modifier and fiber loading. July 26, 2016, http://dx.doi.org/10.1590/0104-1428.2124

[6] Gulmine, J., Janissek, P., Heise, H., & Akcelrud, L. (2002). Polyethylene characterization by FTIR. Polymer Testing, 21(5), 557-563. doi:10.1016/s0142-9418(01)00124-6

[7] Albano de Morais, J., Gadioli, R., & Aurelio De Paoli, M. (2016, June 7). Curaua fiber reinforced high-density polyethylene composites: Effect of impact modifier and fiber loading. July 26, 2016, http://dx.doi.org/10.1590/0104-1428.2124

[8] https://www.eia.gov/tools/faqs/faq.cfm?id=41&t=6

[9] https://www.eia.gov/tools/faqs/faq.cfm?id=38&t=6

[10] http://qz.com/106483/3d-printing-will-explode-in-2014-thanks-to-the-expiration-of-key-patents/

[11] Mahfuz, H., et al., Carbon nanoparticles/whiskers reinforced composites and their tensile response. Composites Part A: Applied Science and Manufacturing, 2004. 35(5): p. 519-527.

[12] Warrior, N.A., et al., The effect of interlaminar toughening strategies on the energy absorption of composite tubes. Composites Part A: Applied Science and Manufacturing, 2004. 35(4): p. 431- 437.

[13] Ivanova, O., C. Williams, and T. Campbell, Additive manufacturing (AM) and nanotechnology: Promises and challenges. Rapid Prototyping Journal, 2013. 19(5): p. 353-364.

[14] Peterson, G.I., et al., 3D-printed mechanochromic materials. ACS Applied Materials and Interfaces, 2015. 7(1): p. 577-583.

[15] Peterson, G.I., et al., Additive manufacturing of mechanochromic polycaprolactone on entry-level systems. Rapid Prototyping Journal, 2015. 21(5): p. 520-527.

[16] Ning, F., et al., Additive manufacturing of carbon fiber reinforced thermoplastic composites using fused deposition modeling. Composites Part B: Engineering, 2015. 80: p. 369-378.

[17] Quan, Z., et al., Microstructural design and additive manufacturing and characterization of 3D orthogonal short carbon fiber/acrylonitrile-butadiene- styrene preform and composite. Composites Science and Technology, 2016. 126: p. 139-148.

[18] Hossain, M.S., et al., Improved Mechanical Properties of Fused Deposition Modeling-Manufactured Parts Through Build Parameter Modifications. Journal of Manufacturing Science and Engineering, Transactions of the ASME, 2014. 136(6).

[19] Nikzad, M., S.H. Masood, and I. Sbarski, Thermo-mechanical properties of a highly filled polymeric composites for Fused Deposition Modeling. Materials and Design, 2011. 32(6): p. 3448-3456.

[20] Wang, J., et al., A novel approach to improve mechanical properties of parts fabricated by fused deposition modeling. Materials and Design, 2016. 105: p. 152-159.

[21] Bellini, A. and S. Guceri, Mechanical characterization of parts fabricated using fused deposition modeling. Rapid Prototyping Journal, 2003. 9(4): p. 252-264.

[22] Domingo-Espin, M., et al., Mechanical property characterization and simulation of fused deposition modeling Polycarbonate parts. Materials and Design, 2015. 83: p. 670-677.

[23] Deffenbaugh, P., Rumph, R. and Church, K., Broadband Microwave Frequency Characterization of 3-D Printed Materials. IEEE Transactions on Components, Packaging and Manufacturing Technology, 2013. p. 2147-2155.

[24] Bagsik, A. and V. Schoppner. Mechanical properties of fused deposition modeling parts manufactured with Ultem*9085. in 69th Annual Technical Conference of the Society of Plastics Engineers 2011, ANTEC 2011, May 1, 2011 - May 5, 2011. 2011. Boston, MA, United states: Society of Plastics Engineers.

[25] Hossain, M.S., et al., Improved Mechanical Properties of Fused Deposition Modeling-Manufactured Parts Through Build Parameter Modifications. Journal of Manufacturing Science and Engineering, Transactions of the ASME, 2014. 136(6).

[26] Kim, D., I.H. Lee, and H.Y. Cho, A study on the mechanical properties of additive manufactured polymer materials. Transactions of the Korean Society of Mechanical Engineers, A, 2015. 39(8): p. 773-780.

[27] Rankouhi, B., et al., Failure Analysis and Mechanical Characterization of 3D Printed ABS With Respect to Layer Thickness and Orientation. Journal of Failure Analysis and Prevention, 2016. 16(3): p. 467-481.

[28] Reese, R., T. Letcher, and M. Rahman, Mechanical Properties of Additively Manufactured Peek Components Using Fused Filament Fabrication. Proceedings of the ASME 2015 International Mechanical Engineering Congress and Exposition 2015.

[29] Yang, R., R.R. Mather, and A.F. Fotheringham, Processing, structure, and mechanical properties of as-spun polypropylene filaments - A systematic approach using factorial design and statistical analysis. Journal of Applied Polymer Science, 2005. 96(1): p. 144-154.

[30] Ameta, G., et al., Investigating the Role of Geometric Dimensioning and Tolerancing in Additive Manufacturing. Journal of Mechanical Design, Transactions of the ASME, 2015. 137(11).

[31] Domingo-Espin, M., et al., Mechanical property characterization and simulation of fused deposition modeling Polycarbonate parts. Materials and Design, 2015. 83: p. 670-677.

[32] Khoda, A.K.M.B. Build direction for improved process plan in multi-material additive manufacturing. in IIE Annual Conference and Expo 2014, May 31, 2014 - June 3, 2014. 2014. 159, Rue Saint-Antoine Ouest, Montreal, QC, Canada: Institute of Industrial Engineers.

[33] Turner, B.N. and S.A. Gold, A review of melt extrusion additive manufacturing processes: II. Materials, dimensional accuracy, and surface roughness. Rapid Prototyping Journal, 2015. 21(3): p. 250-261.

[34] Song, S., et al. Shape deviation modeling for fused deposition modeling processes. in 2014 IEEE International Conference on Automation Science and Engineering, CASE 2014, August 18, 2014 - August 22, 2014. 2014. Taipei, Taiwan: IEEE Computer Society.

[35] Boschetto, A. and L. Bottini, Accuracy prediction in fused deposition modeling. International Journal of Advanced Manufacturing Technology, 2014. 73(5-8): p. 913-928.

[36] Boschetto, A. and L. Bottini, Design for manufacturing of surfaces to improve accuracy in Fused Deposition Modeling. Robotics and Computer-Integrated Manufacturing, 2016. 37: p. 103-114.

[37] Chen, R.K., et al. Nano-CT characterization of structural voids and air bubbles in fused deposition modeling for additive manufacturing. in ASME 2015 International Manufacturing Science and Engineering Conference, MSEC 2015, June 8, 2015 - June 12, 2015. 2015. Charlotte, NC, United states: American Society of Mechanical Engineers.

[38] Lanzotti, A., et al., On the geometric accuracy of RepRap open-source three-dimensional printer. Journal of Mechanical Design, Transactions of the ASME, 2015. 137(10).

[39] Panhalkar, N., R. Paul, and S. Anand, Increasing Part Accuracy in Additive Manufacturing Processes Using a k-d Tree Based Clustered Adaptive Layering. Journal of Manufacturing Science and Engineering, Transactions of the ASME, 2014. 136(6).

[40] Turner, B.N. and S.A. Gold, A review of melt extrusion additive manufacturing processes: II. Materials, dimensional accuracy, and surface roughness. Rapid Prototyping Journal, 2015. 21(3): p. 250-261.

[41] Jin, Y.-a., Y. He, and J.-z. Fu, Support generation for additive manufacturing based on sliced data. International Journal of Advanced Manufacturing Technology, 2015. 80(9-12): p. 2041-2052.

[42] Leary, M., et al., Feasible build orientations for self-supporting fused deposition manufacture: A novel approach to space-filling tesselated geometries. Advanced Materials Research, 2013. 633: p. 148-168.

[43] Volpato, N., J.A. Foggiatto, and D.C. Schwarz, The influence of support base on FDM accuracy in Z. Rapid Prototyping Journal, 2014. 20(3): p. 182-191.

[44] Hu, D., H. Mei, and R. Kovacevic, Improving solid freeform fabrication by laser-based additive manufacturing. Proceedings of the Institution of Mechanical Engineers, Part B: Journal of Engineering Manufacture, 2002. 216(9): p. 1253-1264.

[45] Yang, Y., et al., 3D printing of shape memory polymer for functional part fabrication. International Journal of Advanced Manufacturing Technology, 2016. 84(9-12): p. 2079-2095.

[46] Rankouhi, B., et al., Failure Analysis and Mechanical Characterization of 3D Printed ABS With Respect to Layer Thickness and Orientation. Journal of Failure Analysis and Prevention, 2016. 16(3): p. 467-481.

[47] Reese, R., T. Letcher, and M. Rahman, Mechanical Properties of Additively Manufactured Peek Components Using Fused Filament Fabrication. Proceedings of the ASME 2015 International Mechanical Engineering Congress and Exposition 2015.

[48] ***FORMAT REFERENCE BETTER*** Finite Element Analysis of Composite Materials Using ANSYS®, Second Edition, pg 20-30,

[49] Chen, R.K., et al. Nano-CT characterization of structural voids and air bubbles in fused deposition modeling for additive manufacturing. in ASME 2015 International Manufacturing Science and Engineering Conference, MSEC 2015, June 8, 2015 - June 12, 2015. 2015. Charlotte, NC, United states: American Society of Mechanical Engineers.

[50] Bellini, A. and S. Guceri, Mechanical characterization of parts fabricated using fused deposition modeling. Rapid Prototyping Journal, 2003. 9(4): p. 252-264.

[51] Domingo-Espin, M., et al., Mechanical property characterization and simulation of fused deposition modeling Polycarbonate parts. Materials and Design, 2015. 83: p. 670-677.

[52] Mechanics Of Composite Materials By Robert M. Jones
https://books.google.com/books?id=oMph2kNG3yAC&pg=PA96&dq=Modulus+transformation+relations&hl=en&sa=X&ved=0ahUKEwje5fuQ1JHOAhXKpYMKHaFGA9oQ6AEIWDAJ#v=onepage&q=Modulus%20transformation%20relations&f=false

Notes

Sustainability and 3D printing are two subjects that have been gaining in momentum in the modern world. On one hand constant innovations in manufacturing, like 3D printing, continuously minimize the cost of prototyping and manufacturing leading to higher standards of living and more disposable income for in the economy. On the other hand, all manufacturing leads to waste throughout the product lifecycle. In a way, this project intends to close the product lifecycle loop with thermoplastics and generate a method by which we can manufacture more sustainably. One of the most prevalent materials utilized in manufacturing is petroleum. While most of us recognize the proliferation of petroleum in our lives through our vehicles, the full magnitude of our dependency on petroleum is not a common fact. "Petroleum products include transportation fuels, fuel oils for heating and electricity generation, asphalt and road oil, and the feedstocks used to make chemicals, plastics, and synthetic materials found in *nearly everything* we use today"[8]. FFF is a particularly iconic form of AM and often is what most people think of due to its consumer level accessibility[10]. An FFF printer melts, extrudes, and deposits a filament layer by layer one on top of another to create a product. In FFF 3D printing, one of the most commonly used plastics is Acrylonitrile Butadiene Styrene (ABS), a petroleum-based plastic. It is beloved by the FFF printing community due to its low cost, its thermal and mechanical properties, and its resultant ease of printing compared to other plastics. ABS is also a plastic that takes a protracted amount of time to break down in the environment.

Product design parameters are the parameters that are defined in the CAD and STL files of the product. Product design parameters include parameters such as Build Orientation inside of the Build Chamber[30-33], the Location of the part On the Build Plane[30,34] , Layer Thickness[30,33,35--40], Support Structures[30,41,42,43], and more. Because of the laminar nature of FFF products, the design of the products must consider the mechanical properties of the material (e.g., the maximum hanging angle) as well as the thermal properties (e.g., shrinkage and warping).

Printing process parameters are defined by either physically by the printer or in g-code and are limited by the printer. These parameters include Extruder Diameter[33,49], Deposition Rate[33,34,38,44], Deposition Angle[35,36], Bed Material, and thermal parameters such as Bed Temperature[38,46,47], Extruder Temperature[33,45-47], and Build Environment Chamber Temperature[33]. Printing process parameters must consider both the effects of mechanical properties on printing reliability (if a filament is too brittle or too flexible the printing speed must be reduced) as well as the thermal properties (e.g., cooling rate and warping).